$\bar{K}NN$ quasibound state and the $\bar{K}N$ interaction: Coupled-channels Faddeev calculations of the $\bar{K}NN$-$\pi\Sigma N$ system

N. V. Shevchenko,[1,*] A. Gal,[2] J. Mareš,[1] and J. Révai[3]
[1]*Nuclear Physics Institute, 25068 Řež, Czech Republic*
[2]*Racah Institute of Physics, The Hebrew University, Jerusalem 91904, Israel*
[3]*Research Institute for Particle and Nuclear Physics, H-1525 Budapest, P.O.B. 49, Hungary*
(Received 2 July 2007; published 10 October 2007)

Coupled-channels three-body calculations of an $I = 1/2$, $J^\pi = 0^-$ $\bar{K}NN$ quasibound state in the $\bar{K}NN$-$\pi\Sigma N$ system were performed and the dependence of the resulting three-body energy on the two-body $\bar{K}N$-$\pi\Sigma$ interaction was investigated. Earlier results of binding energy $B_{K^-pp} \sim 50$–70 MeV and width $\Gamma_{K^-pp} \sim 100$ MeV are confirmed [N. V. Shevchenko *et al.*, Phys. Rev. Lett. **98**, 082301 (2007)]. It is shown that a suitably constructed energy-independent complex $\bar{K}N$ potential gives a considerably shallower and narrower three-body quasibound state than the full coupled-channels calculation. Comparison with other calculations is made.

DOI: 10.1103/PhysRevC.76.044004 PACS number(s): 21.45.+v, 11.80.Jy, 13.75.Jz, 24.10.Eq

I. INTRODUCTION

Hadronic nuclei are useful tools for studying hadron-nucleon interactions and in-medium properties of hadrons. The recent interest in kaonic nuclei was motivated by the strongly attractive antikaon-nucleus density-dependent optical potentials obtained from K^- atomic data fits [1]. Akaishi and Yamazaki [2] using G-matrix one-channel $\bar{K}N$ interactions, predicted the existence of deep and narrow K^- bound states in ^{3}He, ^{4}He, and ^{8}Be. Of particular interest is the lightest possible antikaon-nucleus system, K^-pp, for which these authors calculated in Ref. [3] values of 48 and 61 MeV for the total binding energy and the decay width, respectively. Deeply bound kaonic states were searched in ^{4}He(K^-, N) reactions at KEK, with negative results so far [4], and by the FINUDA spectrometer Collaboration at DAΦNE [5] in stopped K^- reactions on nuclear targets such as lithium and carbon. The latter experiment suggested evidence for a bound state K^-pp "observed" through its decay into approximately back-to-back Λ-proton pairs. The deduced binding energy (115 MeV), but not the width (67 MeV), differs considerably from the theoretical prediction of Ref. [3]. However, this interpretation of the measured Λ-proton spectrum in the FINUDA experiment was challenged by Magas *et al.* [6], who also criticized the Yamazaki-Akaishi calculations [3] for using an effective $\bar{K}$ optical potential in lieu of genuine $\bar{K}N$ interactions.

The near-threshold $\bar{K}N$ interaction is mainly affected by the subthreshold $I = 0$ resonance Λ(1405), which is usually assumed a $\bar{K}N$ bound state and a resonance in the $\pi\Sigma$ channel. Numerous theoretical works were devoted to constructing $\bar{K}N$ interactions within K-matrix models, dispersion relations, meson-exchange models, quark models, and cloudy bag-models and more recently by applying SU(3) meson-baryon chiral perturbation theory (see, e.g., the recent review articles [7,8]). Scattering experiments for K^-p are rather old and the data are not too accurate. Kaonic hydrogen provides additional information. Namely, there are two experimental measurements of the $1s$ level shift and width caused by the strong interaction, performed at KEK [9] and recently by the DEAR Collaboration at DAΦNE, Frascati [10]. The measured upward shift appears as due to a repulsive strong interaction, but in fact it is caused by an attractive interaction in the $I = 0$ $\bar{K}N$-$\pi\Sigma$ channel, which is strong enough to generate a quasibound strong-interaction state. The effect of such a strong attractive interaction is to push the purely Coulomb level upward. Using the Deser formula [11], it is possible to obtain the K^-p scattering length from the value of the $1s$ level energy shift. Unfortunately, several recent theoretical models could not simultaneously reproduce the DEAR value of the K^-p scattering length together with the bulk of K^-p scattering data [12].

As should be clear from this brief introduction, the fields of $\bar{K}N$ and $\bar{K}$-nucleus interaction are abundant with open questions and problems. The elucidation of $\bar{K}$-nuclear properties would help considerably to derive significant information on the in-medium $\bar{K}N$ interaction and on the possibility of kaon condensation in dense nuclear matter, see Refs. [13,14] and previous works cited therein. Among $\bar{K}$-nuclear systems, the study of three-body "exotic" systems offers the advantage that Faddeev equations [15], which exactly describe the dynamics of few particles, provide a proper theoretical and computational framework. In the present work, we have generalized the Faddeev equations in the Alt-Grassberger-Sandhas form [16] to include additional "particle" channels and thus performed the first genuinely three-body $\bar{K}NN$-$\pi\Sigma N$ coupled-channels Faddeev calculation in search for quasibound states in the K^-pp system. A preliminary report of this work was given in Ref. [17]. The present article provides a more detailed and complete version of the previous one, especially concerning the dependence of the three-body results on the two-body input. The main result of Ref. [17] is reconfirmed, namely that a single K^-pp $I = 1/2$, $J^\pi = 0^-$ quasibound state exists with binding energy $B \sim 50$–70 MeV and width $\Gamma \sim 100$ MeV. It is shown that "equivalent" single-channel $\bar{K}NN$ calculations of the type reported

*Corresponding author: shevchenko@ujf.cas.cz

by Yamazaki and Akaishi [3] underestimate considerably the binding energy and particularly the width resulting within the full $\bar{K}NN$-$\pi\Sigma N$ coupled-channels calculations.

The article is organized as follows: in Sec. II we describe the derivation of the coupled-channels Faddeev equations in the AGS form. The two-body potentials that enter these equations are described in Sec. III. Results are given in Sec. IV for the full coupled-channels calculations, along with suitably chosen single-channel calculations that could provide a testground for comparison with the single-channel calculation of Ref. [3]. Conclusions are given in Sec. V.

II. FORMALISM

Three-body Faddeev equations [15] in the Alt-Grassberger-Sandhas (AGS) form [16]

$$U_{ij} = (1-\delta_{ij})G_0^{-1} + \sum_{k=1}^{3}(1-\delta_{ik})\,T_k G_0 U_{kj} \qquad (1)$$

define unknown operators U_{ij}, describing the elastic and rearrangement processes $j+(ki)\to i+(jk)$. The inputs for the AGS system of equations (1) are two-body T-matrices, immersed into three-body space. The operator G_0 is the free three-body Green's function. Faddeev partition indices $i, j = 1, 2, 3$ denote simultaneously an interacting pair and a spectator particle. When the initial state is known, as is usually assumed, the system (1) consists of three equations.

The AGS equations are quantum-mechanical ones, describing processes in which the number and composition of particles are fixed. However, the two-body $\bar{K}N$ interaction, which is essential for the K^-pp quasi-bound-state calculation, is strongly coupled to other channels, particulary to the $\pi\Sigma$ channel via $\Lambda(1405)$. To take the $\bar{K}N$-$\pi\Sigma$ coupling directly into account (we neglect the weaker coupled $I=1$ $\pi\Lambda$ channel), it is necessary to extend the formalism of Faddeev equations. To this end it is assumed that in addition to the usual Faddeev channels, which represent different partitions of the same set of particles, there are also "particle" channels. Each of the three "particle" channels consists of three usual Faddeev partitions (here we treat the two nucleons as distinguishable particles, with proper antisymmetrization introduced at a later stage). Thus, all three-body operators will have "particle" indices (α) for each state in addition to the usual Faddeev indices (i), see Table I.

All operators in Eq. (1) now act in this additional "particle" space: T_i transform to $T_i^{\alpha\beta}$, $G_0 \to G_0^{\alpha\beta}$, and $U_{ij} \to U_{ij}^{\alpha\beta}$ ($\alpha, \beta = 1, 2, 3$). The two-body T-matrices have the following form:

$$T_1 \to \begin{pmatrix} T_1^{NN} & 0 & 0 \\ 0 & T_1^{\Sigma N} & 0 \\ 0 & 0 & T_1^{\Sigma N} \end{pmatrix}, \quad T_2 \to \begin{pmatrix} T_2^{KK} & 0 & T_2^{K\pi} \\ 0 & T_2^{\pi N} & 0 \\ T_2^{\pi K} & 0 & T_2^{\pi\pi} \end{pmatrix},$$
$$T_3 \to \begin{pmatrix} T_3^{KK} & T_3^{K\pi} & 0 \\ T_3^{\pi K} & T_3^{\pi\pi} & 0 \\ 0 & 0 & T_3^{\pi N} \end{pmatrix}, \qquad (2)$$

where T_i^{NN}, $T_i^{\pi N}$, and $T_i^{\Sigma N}$ are the usual one-channel two-body T-matrices in three-body space, describing NN, πN, and ΣN interactions, respectively. The elements of the coupled-channels T-matrix, T_i^{KK}, $T_i^{\pi\pi}$, $T_i^{\pi K}$, and $T_i^{K\pi}$, are labeled by two meson indices:

$$T_i^{KK} : \bar{K} + N \to \bar{K} + N$$
$$T_i^{\pi K} : \bar{K} + N \to \pi + \Sigma$$
$$T_i^{K\pi} : \pi + \Sigma \to \bar{K} + N$$
$$T_i^{\pi\pi} : \pi + \Sigma \to \pi + \Sigma.$$

The free Green's function is diagonal in channel indices: $G_0^{\alpha\beta} = \delta_{\alpha\beta}G_0^{\alpha}$, whereas the transition operators $U_{ij}^{\alpha\beta}$ have the most general form.

Searching for quasibound states assumes working at low energies. Low-energy interactions are satisfactorily described by s waves; hence, for all the relevant two-body interactions we use $L_i = 0$. The total orbital angular momentum is then $L = 0$. For the K^-pp system, the total spin is $S = 0$ due to the spin zero of the two protons and spin zero of the K^- meson. All two-body baryon-baryon interactions are then spin-zero interactions. The remaining quantum number is isospin. It is possible to work in either particle or isospin basis, but because the Coulomb interaction is not included in the present calculation and charge independence is assumed for all two-body interactions, it is quite natural to choose the isospin basis. The total isospin I is a conserved quantum number for charge-independent interactions, so a bound (or a quasibound) state must have a definite value of I. For $I = 1/2$ there are two possible (unadmixed) states corresponding to the total spin S of the system. In the $\bar{K}NN$-$\pi\Sigma N$ case S coincides with the spin of the two baryons ($S_i = 0, 1$) and due to their indistinguishability the spin value also fixes the isospin of the two nucleons, $I_{NN} = 1, 0$, respectively. In these states—let us call them pp and d configuration—a more attractive combination of $\bar{K}N$ $I = 0, 1$ forces and a weaker NN singlet force in the pp is competing with a weaker $\bar{K}N$ attraction and a stronger NN triplet force in d. Therefore it is not clear a priori, which of them has a lower energy. We have chosen to calculate the $I = 1/2$, $S = 0$ pp configuration due to its connection to experiment. Moreover, simple isospin recoupling arguments indicate that it might have a lower energy. However, a similar calculation should be performed for the other, $I = 1/2$, $S = 1$ d configuration, too. As for the $I = 3/2$ state, it is governed by a weaker $\bar{K}N$ attraction than the one in the $I = 1/2$ state under consideration in this work.

Separable potentials, and the corresponding T-matrices, are widely used in Faddeev calculations for reducing the

TABLE I. Interacting two-body subsystems for three partition (i) and three "particle" channel (α) indices. The interactions are further labeled by the two-body isospin values, entering the AGS equations with total three-body isospin $I = 1/2$.

$i\backslash\alpha$	$1(\bar{K}NN)$	$2(\pi\Sigma N)$	$3(\pi N\Sigma)$
1	$NN_{I=0,1}$	$\Sigma N_{I=\frac{1}{2},\frac{3}{2}}$	$\Sigma N_{I=\frac{1}{2},\frac{3}{2}}$
2	$\bar{K}N_{I=0,1}$	$\pi N_{I=\frac{1}{2},\frac{3}{2}}$	$\pi\Sigma_{I=0,1}$
3	$\bar{K}N_{I=0,1}$	$\pi\Sigma_{I=0,1}$	$\pi N_{I=\frac{1}{2},\frac{3}{2}}$

dimension of integrals in the equations. The separable-potential approximation is justified by the fact that the kernels of two-particle equations are of the Hilbert-Schmidt type, at least under suitable conditions on the two-particle interactions [18]. Namely, the separable approximation is valid when each of the two-particle subsystems is dominated by a limited number of bound states or resonances [19]. This condition is satisfied for the "main" two-body interactions entering our system, $\bar{K}N$-$\pi\Sigma$ and NN. For the remaining ΣN and πN interactions we expect weaker contributions to the bound-state complex energy (as already demonstrated for ΣN in Ref. [17]). Hence we use for all two-body potentials a separable form:

$$V^{\alpha\beta}_{i,I} = \lambda^{\alpha\beta}_{i,I} \left|g^{\alpha}_{i,I}\right\rangle\left\langle g^{\beta}_{i,I}\right|, \tag{3}$$

which leads to a separable form of T-matrices:

$$T^{\alpha\beta}_{i,I} = \left|g^{\alpha}_{i,I}\right\rangle \tau^{\alpha\beta}_{i,I} \left\langle g^{\beta}_{i,I}\right|. \tag{4}$$

For $\alpha = \beta$ the corresponding T-matrix coincides with the usual one. With the relation (4), the AGS system (1) can be expressed using new transition and kernel operators:

$$X^{\alpha\beta}_{ij,I_iI_j} = \left\langle g^{\alpha}_{i,I_i}\right| G^{\alpha}_0 U^{\alpha\beta}_{ij,I_iI_j} G^{\beta}_0 \left|g^{\beta}_{j,I_j}\right\rangle, \tag{5}$$

$$Z^{\alpha\beta}_{ij,I_iI_j} = \delta_{\alpha\beta} Z^{\alpha}_{ij,I_iI_j} = \delta_{\alpha\beta}(1-\delta_{ij}) \left\langle g^{\alpha}_{i,I_i}\right| G^{\alpha}_0 \left|g^{\alpha}_{j,I_j}\right\rangle. \tag{6}$$

Substituting isospin-dependent $T^{\alpha\beta}_i$, Z^{α}_{ij}, and $X^{\alpha\beta}_{ij}$ into the AGS system (1) we obtain the following system of operator equations:

$$X^{\alpha\beta}_{ij,I_iI_j} = \delta_{\alpha\beta}\, Z^{\alpha}_{ij,I_iI_j} + \sum_{k=1}^{3}\sum_{\gamma=1}^{3}\sum_{I_k} Z^{\alpha}_{ik,I_iI_k} \tau^{\alpha\gamma}_{k,I_k} X^{\gamma\beta}_{kj,I_kI_j}. \tag{7}$$

The number of equations in the system is defined by the number of possible form factors g^{α}_{i,I_i}. As is seen from Table I, before antisymmetrization our system consists of 18 equations.

Three sets of Jacobi momentum coordinates should be introduced for each "particle" channel α: $|\vec{k}_i{}^{\alpha}, \vec{p}_i{}^{\alpha}\rangle$, $i = 1, 2, 3$, $\alpha = 1, 2, 3$. Here, $\vec{k}_i{}^{\alpha}$ is the center-of-mass momentum of the (jk) pair and $\vec{p}_i{}^{\alpha}$ is the momentum of spectator i with respect to the pair (jk), $i \neq j \neq k$. In these coordinates the three-body free Hamiltonian in the channel α is defined as

$$H^{\alpha}_0 = \frac{\left(k^{\alpha}_i\right)^2}{2m^{\alpha}_{jk}} + \frac{\left(p^{\alpha}_i\right)^2}{2\mu^{\alpha}_i}, \tag{8}$$

where the reduced masses also have "particle" channel indices:

$$m^{\alpha}_{jk} = \frac{m^{\alpha}_j m^{\alpha}_k}{m^{\alpha}_j + m^{\alpha}_k}, \quad \mu^{\alpha}_i = \frac{m^{\alpha}_i\left(m^{\alpha}_j + m^{\alpha}_k\right)}{m^{\alpha}_i + m^{\alpha}_j + m^{\alpha}_k}, \quad i \neq j \neq k. \tag{9}$$

In contrast to the usual AGS formalism we have to use not the kinetic energy but the total energy of the system, including rest masses. We introduce threshold energies: $z^{\alpha}_{\rm th} = \sum_{i=1}^{3} m^{\alpha}_i$, so that the total energy is $z_{\rm tot} = z^{\alpha}_{\rm th} + z^{\alpha}_{\rm kin}$, where $z^{\alpha}_{\rm kin}$ denotes the kinetic energy in channel α. The integrations in Eqs. (5) and (6) are performed over one of the Jacobi momenta, namely, over $\vec{k}_i{}^{\alpha}$, which describes the motion of an interacting pair of particles j and k ($i \neq j \neq k$). Thus, the operators X and Z act on the second momentum, $\vec{p}^{\,\alpha}_i$:

$$\begin{aligned} X^{\alpha\beta}_{ij,I_iI_j} &\to \left\langle \vec{p}_i{}^{\alpha}\right| X^{\alpha\beta}_{ij,I_iI_j}(z_{\rm tot}) \left|\vec{p}_j{}'^{\beta}\right\rangle \\ &= X^{\alpha\beta}_{ij,I_iI_j}\left(\vec{p}_i{}^{\alpha}, \vec{p}_j{}'^{\beta}; z^{\alpha}_{\rm kin} + z^{\alpha}_{\rm th}\right), \end{aligned} \tag{10}$$

$$\begin{aligned} Z^{\alpha}_{ij,I_iI_j} &\to \left\langle \vec{p}_i{}^{\alpha}\right| Z^{\alpha}_{ij,I_iI_j}(z_{\rm tot}) \left|\vec{p}_j{}'^{\alpha}\right\rangle \\ &= Z^{\alpha}_{ij,I_iI_j}\left(\vec{p}_i{}^{\alpha}, \vec{p}_j{}'^{\alpha}; z^{\alpha}_{\rm kin} + z^{\alpha}_{\rm th}\right). \end{aligned} \tag{11}$$

The energy-dependent part of a two-body T-matrix, embedded in the three-body space, is defined by the following relation:

$$\begin{aligned} \tau^{\alpha\beta}_{i,I_i} &\to \left\langle \vec{p}_i{}^{\alpha}\right| \tau^{\alpha\beta}_{i,I_i}(z_{\rm tot}) \left|\vec{p}_j{}'^{\beta}\right\rangle \\ &\equiv \delta_{ij}\delta\left(\vec{p}_i{}^{\alpha} - \vec{p}_j{}'^{\beta}\right) \tau^{\alpha\beta}_{i,I_i}\left[z_{\rm tot} - z^{\alpha}_{\rm th} - \frac{\left(p^{\alpha}_i\right)^2}{2\mu_i}\right]. \end{aligned} \tag{12}$$

It is worth noting that all elements of the two-channel two-body $\bar{K}N$-$\pi\Sigma$ T-matrix depend on the kinetic energies in both channels ($z^1_{\rm kin}$ and $z^2_{\rm kin}$) simultaneously. Here we define the argument of the corresponding $\tau^{\alpha\beta}$ using the left "particle" index α. The second kinetic energy can be simply found from the relation $z^{\alpha}_{\rm kin} + z^{\alpha}_{\rm th} = z^{\beta}_{\rm kin} + z^{\beta}_{\rm th}$.

The calculation of the kernels Z involves transformation from one set of Jacobi coordinates to another one and isospin recoupling, using the property of free Green's function:

$$\begin{aligned} \left\langle \vec{p}_i{}^{\alpha}, I^{\alpha}_i\right| G^{\alpha}_0 \left|\vec{p}_j{}'^{\alpha}, I^{\alpha}_j\right\rangle &= \left\langle \vec{p}_i{}^{\alpha}\right| G^{\alpha}_0 \left|\vec{p}_j{}'^{\alpha}\right\rangle_{I^{\alpha}_i I^{\alpha}_j} \\ &\times \left\langle i^{\alpha}_j i^{\alpha}_k\left(I^{\alpha}_i\right) i^{\alpha}_i, I I_z\right| i^{\alpha}_i i^{\alpha}_k\left(I^{\alpha}_j\right) i^{\alpha}_j, I I_z\rangle, \end{aligned} \tag{13}$$

where i^{α}_j and I^{α}_j denote one-particle and two-particle isospins, respectively, with partition subscripts $i \neq j \neq k$, the total three-body isospin and its projection being $I = 1/2$, $I_z = 1/2$.

To search for a resonance or a bound state means to look for a solution of the homogeneous system corresponding to Eq. (7). But before solving the system

$$X^{\alpha}_{i,I_i} = \sum_{k=1}^{3}\sum_{\gamma=1}^{3}\sum_{I_k} Z^{\alpha}_{ik,I_iI_k} \tau^{\alpha\gamma}_{k,I_k} X^{\gamma}_{k,I_k}, \tag{14}$$

we must antisymmetrize operators involving two identical baryons with antisymmetric spin components ($S_i = 0$) and symmetric spatial components ($L_i = 0$). Here, in Eq. (14), and in the following we omit right-hand indices of X: $X^{\alpha\beta}_{ij,I_iI_j} \to X^{\alpha}_{i,I_i}$, which are unnecessary for a homogeneous system. The operator $X^1_{1,0}$ has antisymmetric NN isospin components, so it drops out of the equations. In contrast, the operator $X^1_{1,1}$ has the correct symmetry properties. All the remaining operators form symmetric and antisymmetric pairs, the symmetric ones that are used in the calculation are:

$$\begin{aligned} X^{1,-}_{2,0} &= X^1_{2,0} - X^1_{3,0}, \quad X^{1,+}_{2,1} = X^1_{2,1} + X^1_{3,1}, \\ X^{3,-}_{2,0} &= X^3_{2,0} - X^2_{3,0}, \quad X^{3,+}_{2,1} = X^3_{2,1} + X^2_{3,1}, \\ X^{2,-}_{1,\frac{3}{2}} &= X^2_{1,\frac{3}{2}} - X^3_{1,\frac{3}{2}}, \quad X^{2,+}_{1,\frac{1}{2}} = X^2_{1,\frac{1}{2}} + X^3_{1,\frac{1}{2}}, \\ X^{2,-}_{2,\frac{3}{2}} &= X^2_{2,\frac{3}{2}} - X^3_{3,\frac{3}{2}}, \quad X^{2,+}_{2,\frac{1}{2}} = X^2_{2,\frac{1}{2}} + X^3_{3,\frac{1}{2}}. \end{aligned} \tag{15}$$

Taking into account equalities of some kernel functions, we end up with a system of nine coupled operator equations in the eight new operators (15) and $X^{1}_{1,1}$, all of which have the required symmetry properties. Because the Faddeev equations are dynamical ones, their final number after antisymmetrization corresponds to the number of different form factors entering the interactions. Similar antisymmetrization procedures have been implemented in several multichannel Faddeev calculations, e.g., the fairly recent K^-d work of Ref. [20].

To solve the homogeneous system we transform the integral equations into algebraic ones and then search for the complex energy at which the determinant of the kernel matrix becomes equal to zero. We are looking for a three-body pole, the real part of which is situated between the $\bar{K}NN$ and $\pi\Sigma N$ thresholds, corresponding to a resonance in the $\pi\Sigma N$ channel and a quasibound state (a bound state with nonzero width) in the $\bar{K}NN$ channel. Therefore, we must work on the physical energy sheet of the first channel and on an unphysical sheet of the second channel.

III. INPUT

The separable potential (3), in momentum representation, has a form:

$$V^{\alpha\beta}_{i,I_i}\left(k^{\alpha}_i, k'^{\beta}_i\right) = \lambda^{\alpha\beta}_{i,I_i}\, g^{\alpha}_{i,I_i}\left(k^{\alpha}_i\right) g^{\beta}_{i,I_i}\left(k'^{\beta}_i\right). \tag{16}$$

For the NN, ΣN, and πN interactions we have $\alpha = \beta$, whereas for the coupled-channels $\bar{K}N$-$\pi\Sigma$ interaction $\alpha, \beta = K$ ($\bar{K}N$ channel) or π ($\pi\Sigma$ channel). We constructed our own coupled-channels $\bar{K}N$-$\pi\Sigma$ interactions, plus complex and real one-channel $\bar{K}N$ test potentials discussed below. We also constructed one-channel ΣN interaction and used the PEST NN potential [21]. Here we neglect the πN interaction because its dominant part is in the (3,3) p-wave channel.

A. $\bar{K}N$ interaction

1. Two-channel $\bar{K}N$-$\pi\Sigma$

There are many models of strangeness -1 meson-baryon scattering, constructed using different methods, see, e.g., Refs. [12,22] and references therein. These recent articles describe coupled-channels models of the $\bar{K}N$ interaction, constructed within the framework of chiral perturbation theory. The exclusive use of on-shell amplitudes and the amount of coupled channels involved in such works renders them impractical for Faddeev calculations. We therefore constructed our own potentials for the coupled-channels $\bar{K}N$-$\pi\Sigma$ interaction in the form (16) with form factors

$$g^{\alpha}_{I}(k^{\alpha}) = \frac{1}{(k^{\alpha})^2 + \left(\beta^{\alpha}_{I}\right)^2}. \tag{17}$$

To obtain the parameters $\lambda^{\alpha\beta}_{I}$ and β^{α}_{I} we used the following experimental data:

(i) Mass M_Λ and width Γ_Λ of the $\Lambda(1405)$ resonance, assuming that it is a quasibound state in the $I = 0$ $\bar{K}N$ channel and a resonance in the $I = 0$ $\pi\Sigma$ channel. For the energy of $\Lambda(1405)$ $E_\Lambda = M_\Lambda - \mathrm{i}\,\Gamma_\Lambda/2$, ($c = \hbar = 1$), we adopted the PDG value [23] $E^{\mathrm{PDG}}_{\Lambda} = 1406.5 - \mathrm{i}\,25$ MeV. In some cases we used also other values of M_Λ and Γ_Λ.

(ii) The K^-p scattering length as derived from the atomic $1s$ level shift and width in the KEK experiment [9]

$$a_{K^-p} = (-0.78 \pm 0.15 \pm 0.03) + \mathrm{i}\,(0.49 \pm 0.25 \pm 0.12)\ \mathrm{fm} \tag{18}$$

and in the DEAR Collaboration experiment [10]

$$a_{K^-p} = (-0.468 \pm 0.090 \pm 0.015) + \mathrm{i}\,(0.302 \pm 0.135 \pm 0.036)\ \mathrm{fm}. \tag{19}$$

In the following we denote the KEK value as $a^{\mathrm{KEK}}_{K^-p} = -0.78 + \mathrm{i}\,0.49$ fm and the DEAR value as $a^{\mathrm{DEAR}}_{K^-p} = -0.468 + \mathrm{i}\,0.302$ fm. Due to the fairly large experimental errors and also the large difference between the results of these two measurements, we fitted our parameters to a variety of values for the K^-p scattering length. In Ref. [17] we studied the sensitivity of the Faddeev calculations' results to varying the KEK value within its error bars. The three-body pole energy was found to depend strongly on the input K^-p scattering length. As for the DEAR value of the K^-p scattering length, we note the controversy about its consistency with the bulk of the K^-p scattering data [12,22].

(iii) The very accurately measured threshold branching ratio [24]:

$$\gamma = \frac{\Gamma(K^-p \to \pi^+\Sigma^-)}{\Gamma(K^-p \to \pi^-\Sigma^+)} = 2.36 \pm 0.04. \tag{20}$$

The value 2.36 was used in our fits.

(iv) Elastic $K^-p \to K^-p$ and inelastic $K^-p \to \pi^+\Sigma^-$ total cross sections. We chose these two reactions because among all available cross section data they have sufficient experimental data points with reasonable experimental errors.

We fitted the potential parameters to points (i)–(iii) of this list and then checked how well the resulting potential reproduces the cross sections (iv). The calculated cross sections for four sets of parameters, in comparison with the experimental data, are shown in Figs. 1 and 2. These sets differ from each other by the value of the range parameter β; the remaining parameters were also changed to reproduce the same γ, $a^{\mathrm{KEK}}_{K^-p}$ and $E^{\mathrm{PDG}}_{\Lambda}$ data. We conclude from the figures that the best value of the $\bar{K}N$ range parameter is $\beta = 3.5$ fm^{-1}. In the following we denote the set with $a^{\mathrm{KEK}}_{K^-p}$, $E^{\mathrm{PDG}}_{\Lambda}$, and $\beta = 3.5$ fm^{-1} as the "best set." Figure 3 shows the calculated $I = 0$ elastic $\pi\Sigma$ cross section, demonstrating that $\Lambda(1405)$ is indeed a resonance in this channel.

We were unable to find a value for β, using the DEAR scattering length $a^{\mathrm{DEAR}}_{K^-p}$ and $E^{\mathrm{PDG}}_{\Lambda}$, such that the corresponding set of parameters provided a good description of both cross sections. The elastic $K^-p \to K^-p$ cross sections can be described with $1.5 \leqslant \beta \leqslant 2.5$ fm^{-1}, but the inelastic $K^-p \to \pi^+\Sigma^-$ cross sections for these values are situated much lower

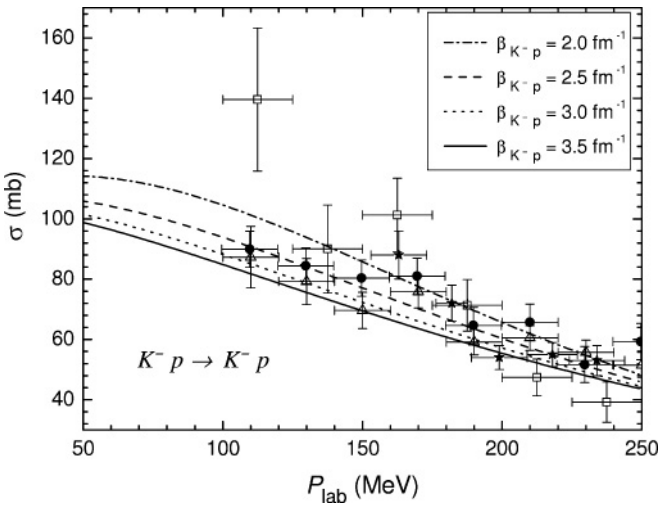

FIG. 1. Total $K^- p \to K^- p$ cross sections calculated for four sets of $\bar{K}N$-$\pi\Sigma$ parameters with different values of β marked in the inset. The experimental values are taken from Refs. [25] (open squares), [26] (open triangles), [27] (solid circles), and [28] (stars).

than the experimental data points. Given this situation, we did not perform three-body calculations with $\bar{K}N$ interaction parameters that reproduce the DEAR value of the $K^- p$ scattering length.

2. *One-channel complex and real $\bar{K}N$*

To investigate all possible dependencies of our three-body results on two-body inputs we constructed additionally real and complex one-channel $\bar{K}N$ potentials. The imaginary part of the complex potential accounts for absorption to all other channels. Both potentials have the same form factors as the coupled-channels potential [Eq. (17)], but for only one channel index $\alpha = \beta = K$. To fit the strength parameters λ

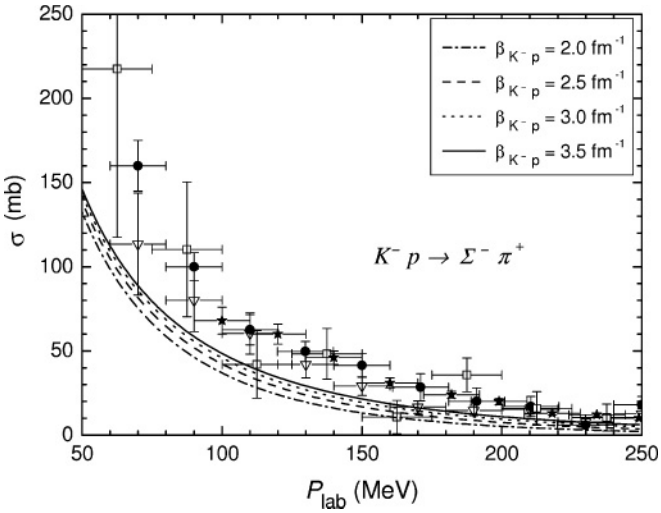

FIG. 2. Total $K^- p \to \pi^+ \Sigma^-$ cross sections calculated for four sets of $\bar{K}N$-$\pi\Sigma$ parameters with different values of β marked in the inset. The experimental values are taken from Refs. [25] (open squares), [26] (open triangles), [27] (solid circles), and [28] (stars).

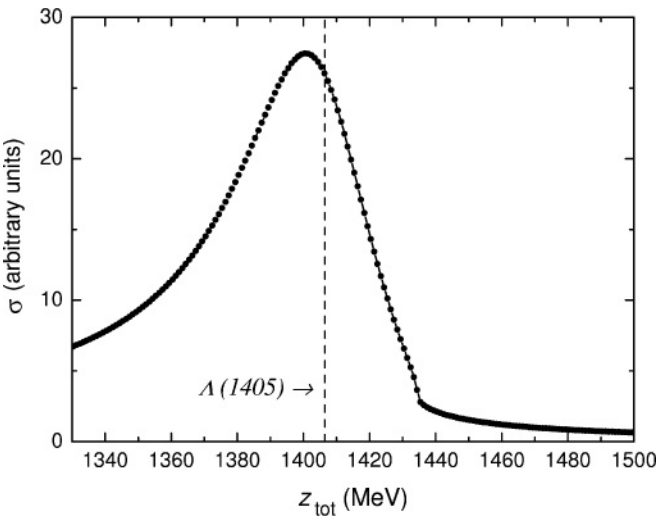

FIG. 3. Calculated elastic $\pi\Sigma$ cross section for $I = 0$, arbitrary units.

of the complex variant, we used experimental data (i) and (ii), i.e., the energy of $\Lambda(1405)$ and $a_{K^- p}$. For the complex $\bar{K}N$ potential we used "best set" plus one more set of data, which is the same as was used in Refs. [2,3]: $E_\Lambda^{\rm AY} = 1405 - i\,20$ MeV, $a_{K^- p}^{\rm AY} = -0.70 + i\,0.53$ fm, and a range parameter $\beta = 1.5$ fm^{-1}. We denote it as "AY set."

A one-channel real $\bar{K}N$ potential was constructed by fitting its parameters to reproduce the real parts of $E_\Lambda^{\rm PDG}$ and $a_{K^- p}^{\rm KEK}$, with $\beta = 3.5$ fm^{-1}. Here we assumed that $\Lambda(1405)$ is a real bound state of the $I = 0$ $\bar{K}N$ subsystem.

B. ΣN interaction

Only few experimental data exist for this interaction. There are different models of it, for example, several Nijmegen models, but due to the lack of data it is not possible to give preference to any of these over the other ones. A separable potential (16) with Yamaguchi form factors

$$g_I^{\Sigma N}(k) = \frac{1}{k^2 + \left(\beta_I^{\Sigma N}\right)^2} \tag{21}$$

was used for the two isospin states. The parameters of the $I = 3/2$ ΣN interaction were fitted to:

(i) the scattering length and effective radius

$$a(I = 3/2) = 3.8 \text{ fm}, \quad r_{\rm eff}(I = 3/2) = 4.0 \text{ fm} \tag{22}$$

from the Nijmegen potential model F [29] (we denote this set of $I = 3/2$ ΣN parameters as ΣN set 1).

(ii) the Nijmegen model NSC97 *YN* phase shifts [30]. This ΣN set 2 gives the following scattering length and effective range:

$$a(I = 3/2) = 4.15 \text{ fm}, \quad r_{\rm eff}(I = 3/2) = 2.4 \text{ fm}. \tag{23}$$

(iii) the scattering length and effective radius

$$a(I = 3/2) = 4.1 \text{ fm}, \quad r_{\rm eff}(I = 3/2) = 3.5 \text{ fm} \tag{24}$$

TABLE II. Three-body pole energy E_{K^-pp} (in MeV) of the $I = 1/2$, $J^\pi = 0^-$ quasibound state of the $\bar{K}NN$ system with respect to the K^-pp threshold calculated with the "best set" of $\bar{K}N$-$\pi\Sigma$ parameters using ΣN set 1, ΣN set 2, ΣN set 3, and with both $I = 1/2$ and $I = 3/2$ ΣN interactions switched off.

ΣN set 1	ΣN set 2	ΣN set 3	no ΣN
$-55.1 - i\,50.9$	$-55.4 - i\,51.9$	$-55.3 - i\,51.1$	$-52.9 - i\,50.9$

from the most recent Nijmegen potential ESC04a [31] (ΣN set 3).

The dependence of the three-body pole position on the ΣN parameters was investigated in Ref. [17]. Table II illustrates the sensitivity of the binding energies and widths of the $I = 1/2$, $J^\pi = 0^-$ quasibound state of the $\bar{K}NN$ system to the ΣN interaction parameters. Due to the weak dependence of the three-body pole position on the ΣN interaction we used in the following only one (the first) set of $I = 3/2$ ΣN parameters.

For the $I = 1/2$ ΣN interaction only the scattering length was approximately determined: $a(I = 1/2) = -0.5$ fm [32]. We fitted the separable-potential parameters to this value, restricting the fit by imposing "natural" values on the parameters and producing a reasonable value for the $I = 1/2$ effective radius.

C. *NN* interaction

We used the nucleon-nucleon PEST potential from Ref. [21], which is a separable approximation of the Paris potential. The strength parameter was set to $\lambda = -1$ and the form factor is:

$$g_I^{NN}(k) = \frac{1}{2\sqrt{\pi}} \sum_{i=1}^{6} \frac{c_{i,I}^{NN}}{k^2 + \left(\beta_{i,I}^{NN}\right)^2}. \tag{25}$$

The constants $c_{i,I}^{NN}$ and $\beta_{i,I}^{NN}$ are listed in Ref. [21]. PEST is on- and off-shell equivalent to the Paris potential up to $E_{\rm lab} \sim 50$ MeV and is repulsive at distances shorter than 0.8 fm. It reproduces the deuteron binding energy $E_{\rm d} = -2.2249$ MeV, as well as the triplet and singlet *NN*-scattering lengths, $a(^3S_1) = -5.422$ fm and $a(^1S_0) = 17.534$ fm, respectively.

IV. RESULTS

A. Results of full coupled-channels $\bar{K}NN$-$\pi\Sigma N$ calculation

Full coupled-channels calculations were done systematically, studying various dependencies of the three-body pole position on different input parameters of the $\bar{K}N$-$\pi\Sigma$ potential. Here the three-body energy is defined as $E_{K^-pp} = -B_{K^-pp} - i\,\Gamma_{K^-pp}/2$, where B_{K^-pp} is a binding energy with respect to the K^-pp threshold, Γ_{K^-pp} is a width of a quasibound state. The dependence of the real and imaginary parts of the three-body pole energy as function of the range parameter β is shown in Figs. 4 and 5, respectively. It is seen that the dependence of the real part on β is rather weak, whereas the imaginary part strongly depends on this parameter.

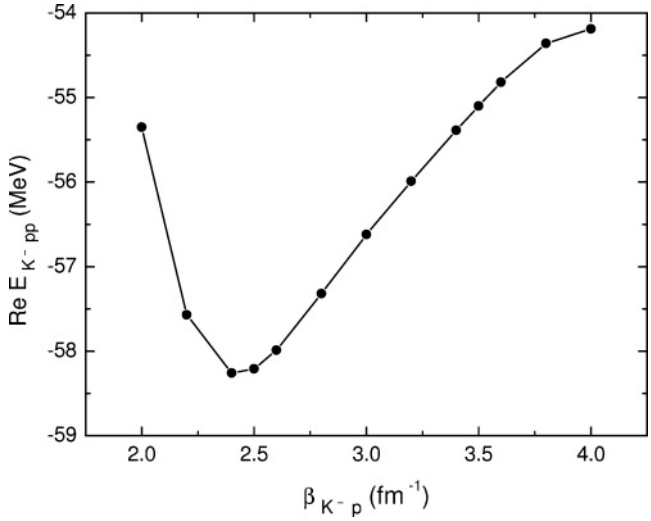

FIG. 4. Coupled-channels calculation: the real part of the three-body $\bar{K}NN$-$\pi\Sigma N$ pole energy as function of the $\bar{K}N$ range parameter β. The two-body $\bar{K}N$-$\pi\Sigma$ observables are fixed at $a_{K^-p}^{\rm KEK}$ and $E_\Lambda^{\rm PDG}$.

Other values that are varied are the mass M_Λ and the width Γ_Λ of the $\Lambda(1405)$ resonance. The results of such variations are shown in Table III. All other input data used in this calculation are fixed at $\beta = 3.5$ fm^{-1} and $a_{K^-p}^{\rm KEK}$. As expected, the broadening of $\Lambda(1405)$ leads to a considerable increase of the three-body width, whereas the three-body binding energy depends on Γ_Λ rather weakly. However, increasing the $\Lambda(1405)$ resonance mass strongly affects both real and imaginary parts of the three-body pole, leading to a fast decrease of both.

B. One-channel real and complex $\bar{K}NN$ calculations

We also performed a test calculation for the one-channel $\bar{K}NN$ system using a one-channel real $\bar{K}N$ potential (T-matrix). For fitting we used the real part of $a_{K^-p}^{\rm KEK}$, the real part of $E_\Lambda^{\rm PDG}$, and assumed $\Lambda(1405)$ as a real bound state of the $I = 0$ $\bar{K}N$ subsystem. For these data, and using $\beta = 3.5$ fm^{-1}, we found a real bound state for $I = 1/2$, $J^\pi = 0^-$ $\bar{K}NN$ at -43.8 MeV below the K^-pp threshold (the first column in Table IV).

Another test calculation was performed with a one-channel complex $\bar{K}N$ potential. The strength parameters λ of the potential were fitted to the $a_{K^-p}^{\rm KEK}$ and $E_\Lambda^{\rm PDG}$ data, and the

TABLE III. Calculated three-body pole energy E_{K^-pp} in MeV, of the $I = 1/2$, $J^\pi = 0^-$ quasibound state of the $\bar{K}NN$ system with respect to the K^-pp threshold, for different two-body input, mass M_Λ and half-width $\Gamma_\Lambda/2$ of the $\Lambda(1405)$. For $E_\Lambda = 1420 - i\,20$ MeV no reasonable $T_{\bar{K}N\text{-}\pi\Sigma}$ parameters can be found.

$\Gamma_\Lambda/2 \backslash M_\Lambda$	1400	1410	1420
20	$-62.1 - i\,46.9$	$-47.5 - i\,37.6$	No $T_{\bar{K}N\text{-}\pi\Sigma}$
25	$-64.9 - i\,58.4$	$-50.8 - i\,47.4$	$-40.6 - i\,39.4$
30	$-65.7 - i\,72.2$	$-52.5 - i\,59.8$	$-42.8 - i\,50.8$

TABLE IV. Results of different calculations of the three-body pole energy E_{K^-pp} in MeV, with respect to the K^-pp threshold: real and complex $\bar{K}NN$ one-channel (first two columns) and full coupled-channels calculations (third column) using the "best set" of $\bar{K}N$-$\pi\Sigma$ parameters. Fourth column: complex $\bar{K}NN$ one-channel calculation with "AY set." Fifth column: AY's result [3].

$E^{\rm best}_{1\,\rm real}$	$E^{\rm best}_{1\,\rm complex}$	$E^{\rm best}_{2\,\rm coupled}$	$E^{\rm AY}_{1\,\rm complex}$	E from Ref. [3]
-43.8	$-40.2 - i\,38.7$	$-55.1 - i\,50.9$	$-46.6 - i\,29.6$	$-48.0 - i\,30.5$

dependence of the three-body pole on the range parameter β was investigated. Results are presented in Fig. 6.

It is seen from the plot that increasing the range of the $\bar{K}N$ interaction, by decreasing the range parameter β, gives rise to a deeper and somewhat narrower three-body level. The dependence of the calculated $\bar{K}NN$ energy on the range parameter β, as displayed in Fig. 6, is rather strong. Therefore, using a too large or a too small range parameter for the complex $\bar{K}N$ interaction leads to substantial underestimate or overestimate, respectively, of the three-body energy. The "best set" of $\bar{K}N$ parameters with a fixed value for the range parameter, $\beta = 3.5$ fm^{-1}, yields the three-body pole energy $E^{\rm best}_{1\,\rm complex}$ shown in the second column of Table IV. The result of the full coupled-channels calculation $E^{\rm best}_{2\,\rm coupled}$ is shown in the third column.

The transition within a three-body single-channel $\bar{K}NN$ calculation from using a real $\bar{K}N$ interaction to using the complex $\bar{K}N$ interaction, fitted to $E^{\rm PDG}_{\Lambda}$ and to $a^{\rm KEK}_{K^-p}$, is demonstrated in Fig. 7 by the trajectory of complex three-body energies starting with the real $E^{\rm best}_{1\,\rm real}$ at the upper-left corner and ending with the complex $E^{\rm best}_{1\,\rm complex}$ at the lower-right corner. This trajectory is generated by varying a real parameter ε between 0 to 1, $\varepsilon = 0$ for $E^{\rm best}_{1\,\rm real}$ and $\varepsilon = 1$ for $E^{\rm best}_{1\,\rm complex}$, such that the imaginary parts of the fitted $E^{\rm PDG}_{\Lambda}$ and $a^{\rm KEK}_{K^-p}$ are scaled down by ε:

$$\mathrm{Im}\, E^{\rm PDG}_{\Lambda} \to \varepsilon\, \mathrm{Im}\, E^{\rm PDG}_{\Lambda}, \quad \mathrm{Im}\, a^{\rm KEK}_{K^-p} \to \varepsilon\, \mathrm{Im}\, a^{\rm KEK}_{K^-p}. \tag{26}$$

It is interesting to note that although the $I = 0$ and $I = 1$ strength parameters $\lambda_{\rm complex}$ provide stronger attraction in the $\bar{K}N$ systems than the attraction provided by $\lambda_{\rm real}$, yet $E_{1\,\rm complex}$ signifies less binding than $E_{1\,\rm real}$. This generalizes the well-known property in two-body problems where including absorptivity leads effectively to adding repulsion. Here we find that absorption of flux from the $\bar{K}N$ channel into other unspecified channels represented by an imaginary part of a complex $\bar{K}N$ potential reduces also the three-body binding energy.

Comparing the result of the one-channel complex $\bar{K}NN$ calculation with the coupled-channels $\bar{K}NN$ (see Table IV) shows that $E_{2\,\rm coupled}$ is much deeper and broader than $E_{1\,\rm complex}$. This means that the $\pi\Sigma$ channel, within a genuinely three-body coupled-channels calculation plays an important dynamical role in forming the three-body resonance (quasibound state), over its obvious role of absorbing flux from the $\bar{K}N$ channel. The poor applicability of an optical potential approach (or some low-order perturbation calculation) in searching for a quasibound state was shown, for example, by Ueda [33], who studied the ηNN-πNN coupled-channels system using Faddeev equations, finding a large deviation of the calculated results from optical-model predictions.

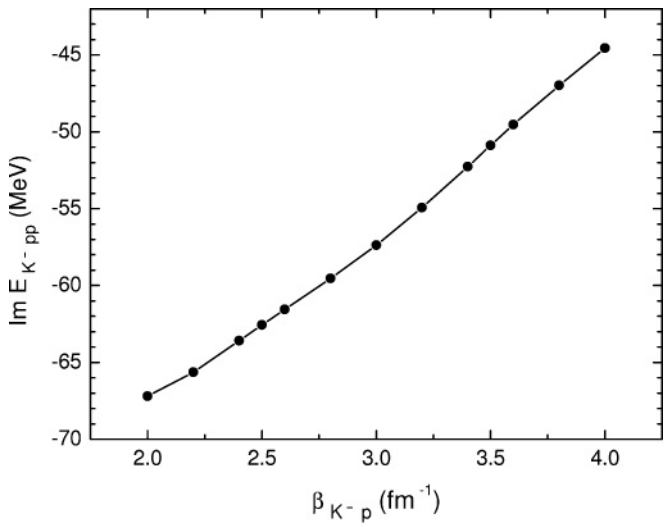

FIG. 5. Coupled-channels calculation: the imaginary part of the three-body $\bar{K}NN$-$\pi\Sigma N$ pole energy as function of the $\bar{K}N$ range parameter β. The two-body $\bar{K}N$-$\pi\Sigma$ observables are fixed at $a^{\rm KEK}_{K^-p}$ and $E^{\rm PDG}_{\Lambda}$.

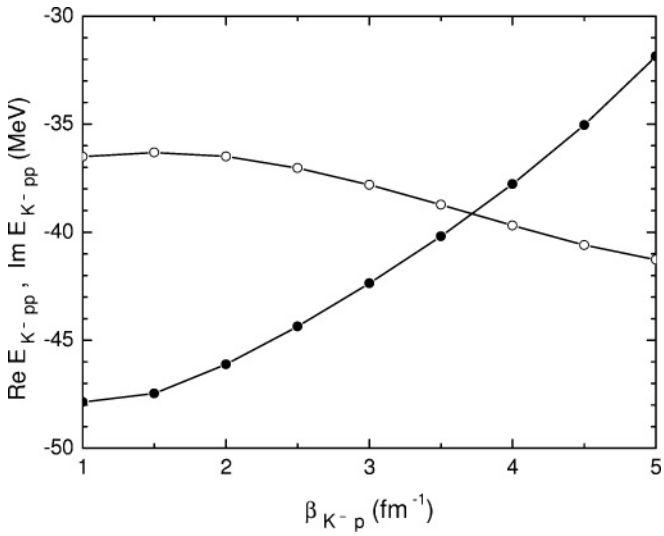

FIG. 6. One-channel calculation with complex $\bar{K}N$ potential: the dependence of the real (solid circles) and imaginary (open circles) parts of three-body $\bar{K}NN$ pole energy on the $\bar{K}N$ range parameter β. The two-body $\bar{K}N$ observables are fixed at $a^{\rm KEK}_{K^-p}$ and $E^{\rm PDG}_{\Lambda}$.

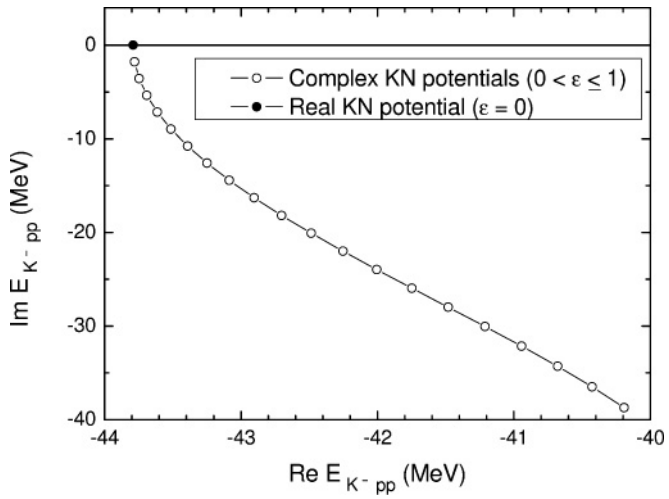

FIG. 7. Trajectory of the three-body pole in the complex energy plane from $E^{\rm best}_{1\,\rm real}$, corresponding to a real $\bar{K}N$ potential with $\varepsilon = 0$ (solid point), to $E^{\rm best}_{1\,\rm complex}$ for a complex $\bar{K}N$ potential with $\varepsilon = 1$ (see text for details).

To compare the present results with the results of calculations by Yamazaki and Akaishi [3], the one-channel $\bar{K}NN$ calculation was repeated using the complex $\bar{K}N$ potential corresponding to the "AY set" of $\bar{K}N$ parameters. The result obtained by us ($E^{\rm AY}_{1\,\rm complex}$) and E from Ref. [3] are shown in the last two columns of Table IV. It is remarkable that in spite of different forms of the two-body potentials and different three-body formalisms, the calculated three-body energies in these single-channel $\bar{K}NN$ calculations come out very close to each other, provided the same set of $\bar{K}N$ parameters is fitted to. Nevertheless, both values of three-body energy are far away from the three-body energy of the complete coupled-channels calculation. One of the reasons is the use of a complex $\bar{K}N$ potential in the single-channel $\bar{K}NN$ calculations, another reason is the too small value, $\beta = 1.5$ fm^{-1}, for the range parameter used in these approximate calculations.

V. CONCLUSION

We performed coupled-channels few-body calculations of the $I = 1/2$, $J^\pi = 0^-$ $\bar{K}NN$ system, finding a deeply bound and broad quasibound state, which is a resonance in the $\pi\Sigma N$ channel. The calculations yielded binding energy $B_{K^-pp} \sim$ 50–70 MeV and width $\Gamma_{K^-pp} \sim 100$ MeV, in agreement with our earlier results [17]. It was shown that the explicit inclusion of the second channel is crucial for this system. The dependence of the three-body energy pole on different forms and parameters of the $\bar{K}N$ interaction, and on different ways of reproducing $\bar{K}N$-$\pi\Sigma$ observables, was studied. Most of these dependencies were found to be strong. In particular, it was shown that a complex $\bar{K}N$ potential gives much shallower and narrower three-body quasibound state than the full coupled-channels calculation, which has the same range parameter and reproduces the same $\bar{K}N$-$\pi\Sigma$ observables.

We compared our results with those of Yamazaki and Akaishi [3], demonstrating the shortcomings of these single-channel $\bar{K}NN$ calculations. Two more calculations of the same system appeared recently. Dote and Weise [34] have presented preliminary results of a variational antisymmetrized molecular dynamics calculation for the K^-pp system within a single-channel $\bar{K}NN$ framework. Their calculation focuses attention to the dependence of the calculated real three-body binding energy on the range parameter of the Gaussian $\bar{K}N$ interaction used. It includes perturbatively also a p-wave $\bar{K}N$ interaction. Whereas a direct comparison between our coupled-channels calculations and these single-channel calculations cannot be made, the general criticism expressed above of the use of a single-channel formalism applies also to this work.

A coupled-channels $\bar{K}NN$-$\pi\Sigma N$ calculation of the same K^-pp system was performed recently by Ikeda and Sato [35] with less emphasis on reproducing low-energy $\bar{K}N$ data. The obtained binding energies are in a similar range to those presented here, whereas the widths are consistently lower than those calculated in the present work.

It is worthwhile to note that all the theoretical calculations discussed above, including the present calculations, obtain binding energies that are considerably below the binding energy $\approx$115 MeV deduced for the K^-pp identification proposed in Ref. [5]. This FINUDA $K^-_{\rm stop}$ experiment on lithium and heavier targets, as mentioned in the Introduction, leaves room for other interpretations as well. The use of a more restrictive ^{3}He target to search for a K^-pp quasibound state in a (K^-, n) reaction was approved as a "day 1" experiment in J-PARC [36]. The spectrum calculated recently for this reaction [37] demonstrates how the large width predicted for K^-pp in the present work is expected to wipe out any clear peak structure in this reaction.

Additional calculations are necessary to study other features of the coupled $\bar{K}NN$ system. These include the secondary effect of the $\pi\Lambda$ channel beyond that of the primary inelastic $\pi\Sigma$ channel incorporated here, of p-wave $\bar{K}N$ and πN interactions, and the use of relativistic kinematics. Finally, to understand better the $\bar{K}N$ interaction, it is desirable to perform coupled-channels Faddeev calculations of a quasibound state in the $S = 1$ $\bar{K}NN$ system as well.

ACKNOWLEDGMENTS

The work was supported by the Czech GA AVCR grant A100480617 and by the Israel Science Foundation grant 757/05.

[1] E. Friedman, A. Gal, and C. J. Batty, Phys. Lett. **B308**, 6 (1993); Nucl. Phys. **A579**, 518 (1994); C. J. Batty, E. Friedman, and A. Gal, Phys. Rep. **287**, 385 (1997); A. Cieplý, E. Friedman, A. Gal, and J. Mareš, Nucl. Phys. **A696**, 173 (2001); J. Mareš, E. Friedman, and A. Gal, *ibid*. **A770**, 84 (2006).
[2] Y. Akaishi and T. Yamazaki, Frascati Phys. Ser. **16**, 59 (1999); Phys. Rev. C **65**, 044005 (2002).
[3] T. Yamazaki and Y. Akaishi, Phys. Lett. **B535**, 70 (2002).
[4] M. Iwasaki *et al*., arXiv:0706.0297 [nucl-ex].
[5] M. Agnello *et al*., Phys. Rev. Lett. **94**, 212303 (2005).

[6] V. K. Magas, E. Oset, A. Ramos, and H. Toki, Phys. Rev. C **74**, 025206 (2006).
[7] J. A. Oller, J. Prades, and M. Verbeni, Eur. Phys. J. A **31**, 527 (2007).
[8] W. Weise, arXiv:nucl-th/0701035.
[9] M. Iwasaki *et al*., Phys. Rev. Lett. **78**, 3067 (1997); T. M. Ito *et al*., Phys. Rev. C **58**, 2366 (1998).
[10] G. Beer *et al*., Phys. Rev. Lett. **94**, 212302 (2005).
[11] S. Deser *et al*., Phys. Rev. **96**, 774 (1954); T. L. Trueman, Nucl. Phys. **26**, 57 (1961).
[12] B. Borasoy, R. Nißler, and W. Weise, Phys. Rev. Lett. **94**, 213401 (2005); **96**, 199201 (2006); Eur. Phys. J. A **25**, 79 (2005); B. Borasoy, U.-G. Meißner, and R. Nißler, Phys. Rev. C **74**, 055201 (2006).
[13] G. E. Brown, C.-H. Lee, H.-J. Park, and M. Rho, Phys. Rev. Lett. **96**, 062303 (2006).
[14] Y. Kim, K. Kubodera, D.-P. Min, F. Myhrer, and M. Rho, Nucl. Phys. **A792**, 249 (2007).
[15] L. D. Faddeev, Sov. Phys. JETP **12**, 1014 (1961); Mathematical aspects of the three-body problem in quantum scattering theory, Steklov Math. Institute 69 (1963).
[16] E. O. Alt, P. Grassberger, and W. Sandhas, Nucl. Phys. **B2**, 167 (1967).
[17] N. V. Shevchenko, A. Gal, and J. Mareš, Phys. Rev. Lett. **98**, 082301 (2007).
[18] K. Meetz, J. Math. Phys. **3**, 690 (1962).
[19] C. Lovelace, Phys. Rev. **135**, B1225 (1964).
[20] A. Bahaoui, C. Fayard, T. Mizutani, and B. Saghai, Phys. Rev. C **68**, 064001 (2003).
[21] H. Zankel, W. Plessas, and J. Haidenbauer, Phys. Rev. C **28**, 538 (1983).
[22] J. A. Oller, J. Prades, and M. Verbeni, Phys. Rev. Lett. **95**, 172502 (2005); **96**, 199202 (2006); J. A. Oller, Eur. Phys. J. A **28**, 63 (2006).
[23] W.-M. Yao *et al*. (Particle Data Group), J. Phys. G **33**, 1 (2006).
[24] D. N. Tovee *et al*., Nucl. Phys. **B33**, 493 (1971); R. J. Nowak *et al*., *ibid*. **B139**, 61 (1978).
[25] W. E. Humphrey and R. R. Ross, Phys. Rev. **127**, 1305 (1962).
[26] M. Sakitt *et al*., Phys. Rev. **139**, B719 (1965).
[27] J. K. Kim, Phys. Rev. Lett. **14**, 29 (1965); Columbia University Report, Nevis 149 (1966); **19**, 1074 (1967).
[28] J. Ciborowski *et al*., J. Phys. G **8**, 13 (1982).
[29] M. M. Nagels, Th. A. Rijken, and J. J. de Swart, Phys. Rev. D **20**, 1633 (1979).
[30] http://nn-online.org by the Nijmegen group.
[31] Th. A. Rijken and Y. Yamamoto, Phys. Rev. C **73**, 044008 (2006).
[32] R. H. Dalitz, Nucl. Phys. **A354**, 101c (1981).
[33] T. Ueda, Phys. Rev. Lett. **66**, 297 (1991).
[34] A. Dote and W. Weise, arXiv:nucl-th/0701050.
[35] Y. Ikeda and T. Sato, arXiv:nucl-th/0701001; Phys. Rev. C **76**, 035203 (2007).
[36] T. Nagae, *Spectroscopy of Hypernuclei with Meson Beams*, in *Topics in Strangeness Nuclear Physics*, Lecture Notes in Physics 724, edited by P. Bydzovsky, A. Gal, and J. Mares (Springer, Berlin Heidelberg, 2007), pp. 81–111.
[37] T. Koike and T. Harada, Phys. Lett. **B652**, 262 (2007) .